The influence of atomic ordering on strain relaxation during the growth of metamorphic solar cells

A G Norman, R M France, W E McMahon, J F Geisz and M J Romero

National Renewable Energy Laboratory, 15013 Denver West Parkway, Golden CO 80401, USA

E-mail: andrew.norman@nrel.gov

Abstract. The occurrence of single variant $CuPt_B$ ordering during growth of InGaP graded buffer layer structures on offcut (001) GaAs substrates for inverted metamorphic solar cells is found to have a strong influence on strain relaxation mechanisms. Since the surface-induced $CuPt_B$ ordering is metastable in the bulk of the material, a strong preference is observed for the nucleation and glide of 60° type misfit dislocations with Burgers vectors that introduce an antiphase boundary into the ordered structure. This results in an overall epitaxial layer tilt in the opposite sense to that normally observed for the direction of substrate offcut. Furthermore, in InGaP buffer layers graded to InP, a switch in the dislocation glide plane preference back to that normally observed for the direction of substrate offcut is observed as the degree of atomic ordering falls below a critical value. This results in the nucleation and glide of new misfit dislocations resulting in an increase in the threading dislocation density that is found to have a deleterious effect on device efficiency. Understanding the materials science behind this behavior will enable the engineering of more effective, lower threading dislocation density strain relief buffer layers resulting in improved performance of subsequently grown devices.

1. Introduction

The growth of lattice-mismatched semiconductor heterostructures introduces increased degrees of freedom in the design of optoelectronic devices for desired properties such as emission wavelength of light emitting diodes and optimal band gap combinations for ultra-high efficiency multijunction solar cells. Fundamental to the achievement of the highest performance devices is an understanding of the factors that affect strain relaxation processes that occur during the epitaxial growth of these lattice-mismatched layer structures, such as dislocation nucleation and glide, and epitaxial layer tilt.

The highest efficiency solar cells so far produced are multijunction solar cells that are typically operated under concentrated light. There are presently two main approaches to producing this type of cell: (i) an all lattice-matched approach using a dilute III-nitride alloy as an ≈1 eV junction [1], or (ii) a metamorphic approach where one or more of the junctions are lattice-mismatched with respect to the substrate used for growth [2–7]. Both of these methods have resulted in multijunction solar cells with efficiencies greater than 40 % under concentrated light. Multijunction solar cells are able to reach such high efficiencies because their design reduces the thermalization and transmission losses that are typically associated with single junction devices and hence enables a fuller utilization of the solar spectrum [e.g., 8]. However, to produce such high efficiency devices requires extremely high quality, epitaxial III-V semiconductor materials. These can only be grown on very expensive single crystal substrates using costly epitaxial growth techniques. In order to reduce costs, multijunction solar cells

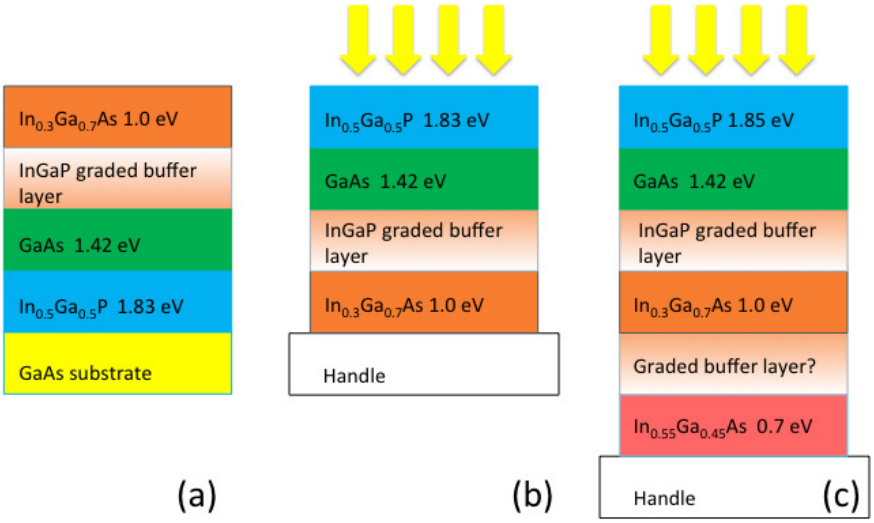

Figure 1. Schematic showing IMM solar cells. (a) Triple-junction device as grown on GaAs substrate. (b) Triple-junction device after flipping the structure over, bonding to a suitable handle, and removal of the substrate. (c) Four-junction device.

for terrestrial applications are generally used in a concentrator system where the light is gathered from a large area and then focused using a relatively cheap optical element onto a very small area multijunction solar cell. An added bonus is that the efficiency of the multijunction solar cells generally increases under concentrated light [e.g., 9].

The particular structure being investigated at NREL is the inverted metamorphic multijunction (IMM) solar cell [2, 4, 5]. A schematic showing this structure is shown in figure 1. An efficiency of 42.6 % has recently been reported for this triple-junction device structure and >44% efficiency is expected after further optimization [10]. However, further significant efficiency gains beyond this are only likely to be obtained by the addition of a fourth junction with a band gap of ≈ 0.7 eV, figure 1(c) [e.g., 11]. The IMM solar cell has several advantages over the upright lattice-matched and upright metamorphic multijunction (MM) solar cells. The first is that a wider range of band gaps is potentially available for the metamorphic approach than for the lattice-matched approach, figure 2. In the IMM design, the two most power producing high band gap junctions are lattice-matched and hence a higher efficiency may be expected due to a lower sensitivity to the presence of mismatched-induced defects than in the case of the upright MM solar cell where the high band gap junctions are lattice-mismatched. The IMM design also has the potential for a large cost reduction by enabling substrate reuse after removal of the cell active layers that may also be bonded to a handle material with more favorable properties than the original substrate, such as a lighter weight or flexibility. However, to obtain the highest efficiency IMM solar cells require the growth of highly perfect, transparent, graded buffer layers to minimize optical losses and recombination losses associated with the introduction of structural defects such as dislocations resulting from the lattice-mismatch.

To achieve the four-junction IMM device illustrated in figure 1, we are developing a graded InGaP buffer layer structure to step the lattice parameter from that of 1.0 eV band gap InGaAs to that of 0.7 eV InGaAs, figure 2. For this application the InGaP graded buffer layer must be transparent to photons with energies between 0.7 eV and 1.0 eV and also be electrically conducting. It is also essential to promote dislocation glide during growth of this graded buffer layer to minimize the density of threading dislocations that would have a deleterious effect on the efficiency of the final device. Strain relaxation in lattice-mismatched III-V semiconductor epitaxial growth normally occurs by the nucleation and glide of 60° type misfit dislocations once a certain critical thickness has been exceeded. These misfit dislocations generally lie along the orthogonal <110> directions at the interfaces between layers in samples grown on (001) substrates and their $a/2$<011> Burgers vectors are at an angle of 60°

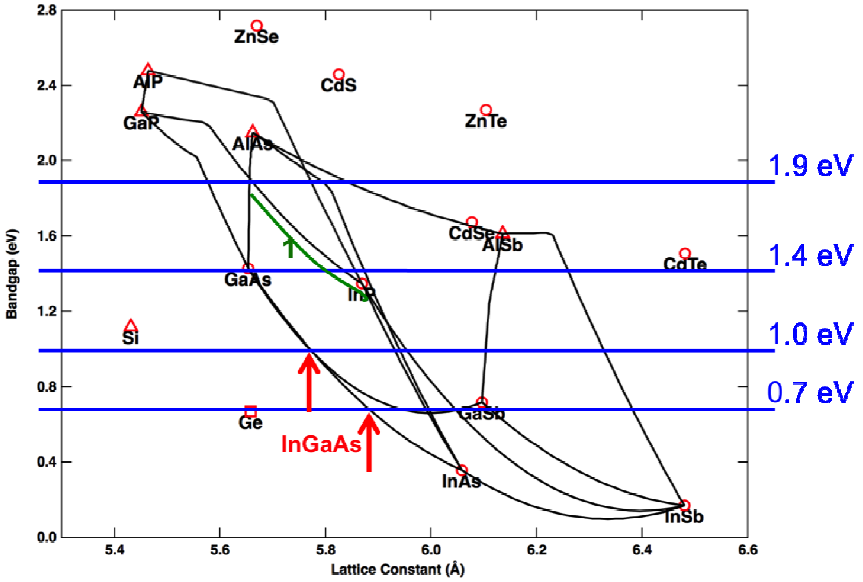

Figure 2. Band gap versus lattice parameter plot for selected group IV, III-V, and II-VI semiconductors showing lattice-mismatched InGaAs junction materials of band gaps 1.0 and 0.7 eV and a potential graded buffer layer path, 1, using InGaP alloys between the lattice parameters of GaAs and these two InGaAs alloys.

to the <110> line direction of the dislocations, and at 45° to the interface, as shown in figure 3 [12]. These dislocations possess screw, misfit, and tilt components and glide on {111} planes. Depending on the sign of the strain and the <110>-line direction, these dislocations can either have group V atoms at the core, α-dislocations, or group III atoms at the core, β-dislocations. For the InGaP compressively strained graded buffer layer of interest in this work, α-dislocations have a line vector of [1-10], whilst β-dislocations have a line vector of [110]. It should also be noted that these 60° type glide dislocations are frequently observed to dissociate into two Shockley partial dislocations separated by an intrinsic stacking fault [13, 14]. The possible slip systems for 60° dislocations in the compressively strained InGaP semiconductor alloy are listed in table I together with the dislocation line vectors, Burgers vectors and components, slip planes and dislocation type [15].

Under the growth conditions normally used, the InGaP graded buffer layers are found to atomically order on {111}B planes [16–18]. This $CuPt_B$ form of ordering is predicted to be energetically unstable in the bulk of the material but is found to be energetically favorable during growth on a reconstructed surface containing [110] rows of [-110]-oriented P dimers [19–21]. On exact (001) oriented substrates, a mixture of the two {111}B variants is observed but a preferential selection of a single variant can be obtained by growth on a substrate offcut a few degrees from (001) towards one of the {111}B planes [21]. Since the ordered planes are {111}, the same as the preferred glide planes for 60° misfit dislocations in zincblende III-V semiconductors, this has important consequences on the dislocation nucleation and glide behavior and strain relaxation mechanisms in these graded buffer layer structures. Depending on the Burgers vector, certain of the 60° misfit dislocations will leave behind an antiphase boundary (APB) in the ordered structure as they glide [16, 17, 22], see table 1. Since the ordered structure is metastable in the bulk, this results in a net reduction in the energy of the layer giving an energetic preference for the nucleation and glide of misfit dislocations that produce APBs. We present experimental results that illustrate this behavior and discuss the consequences it has for strain relaxation in these graded buffer layer systems and what effect it might have on the resulting threading dislocation density.

2. Experimental Procedures

InGaP layers and compositionally graded buffer layers were grown on (001) GaAs substrates offcut by 2° towards one of the {111}B planes by atmospheric pressure metal organic vapor phase epitaxy (MOVPE). The InGaP layers were grown at 675° C. Transmission electron microscope (TEM) cross-section samples were typically prepared by standard mechanical polishing and dimpling techniques followed by argon ion milling with the sample rotated and cooled by liquid nitrogen to preserve the atomic ordering that was normally present. A few samples were prepared in an FEI dual beam FIB workstation using a lift out technique. Cross-section TEM and transmission electron diffraction (TED) experiments were performed in an FEI ST 30 TEM operated at 300 kV. Threading dislocation density was measured by cathodoluminescence (CL) imaging in a JEOL 5800 scanning electron microscope (SEM) equipped with Ge and InGaAs detectors. Epitaxial layer tilt, misfit, and strain relaxation of the samples were measured by high-resolution x-ray diffraction (XRD) reciprocal space mapping (RSM) using a Bede D1 diffractometer.

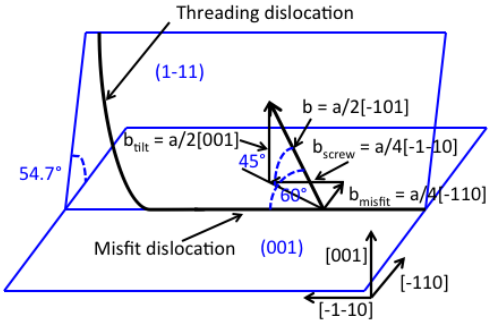

Figure 3. Diagram illustrating the nature of the typically observed 60° type misfit dislocation and associated threading dislocation in zincblende III-V semiconductors.

3. Experimental Results

Figure 4 illustrates TEM, TED, and XRD RSM results obtained from an InGaP step-graded buffer layer, grown on an (001) GaAs substrate offcut 2° towards (-111), where the lattice parameter was graded from that of GaAs to that of InP. In the 220 dark field (DF) image of figure 4(a) the array of 60° misfit dislocations that are introduced to relieve the strain during the growth of this structure can clearly be seen. The InP layer grown on top of the graded buffer layer contains a threading dislocation density ≈ 2.2 x 10^7 cm^{-2}, showing the potential of the graded buffer layer technique for reducing the density of harmful threading defects in the device structure that is typically grown above. In figure 4(b), selected area TED patterns, obtained from < 1μm areas of the sample, are shown of the InGaP graded buffer layer at various positions through the structure. Strong ½{-111} superlattice spots are observed in the first few InGaP layers whose composition is close to 50% Ga, indicating the presence of strong single variant $CuPt_B$ ordering in the alloy. The single variant nature of the ordering is a consequence of the growth on an offcut substrate, 2° towards (111)B, that is typically used in MOVPE to obtain improved quality material. As the InGaP alloy composition becomes more In-rich the maximum degree of atomic ordering possible decreases linearly to zero at InP and this is visible in the TED patterns as a gradual disappearance of the ½{111} superlattice spots as the alloy approaches the InP rich region. The XRD RSM of this sample shown in figure 4(c) shows several interesting features. First, the growth of the InGaP graded buffer layer results in the generation of a significant epitaxial layer tilt indicating an imbalance in the density of misfit dislocations that have nucleated and glided into the material on the (-111) and (1-11) planes. The second interesting point is that the sense of the layer tilt is in the opposite direction to that expected for the substrate offcut. The third interesting feature is that as the InGaP graded buffer layer composition approaches InP, eventually the sense of the overall epitaxial layer tilt begins to reverse back to that normally expected for the substrate offcut and this seems to correlate with the disappearance of the atomic ordering. This change in the epitaxial layer tilt is associated with a switch in the preferred {111} glide plane of the misfit dislocations and results in a sudden increase in the threading dislocation density above this point that is harmful to any device grown on such a buffer layer structure [22].

Table 1. Details of possible slip systems and 60° degree misfit dislocations possible in compressively strained InGaP layers grown on a (001) substrate.

Slip System	Line Direction	Burgers vector	b_{misfit}	b_{screw}	b_{tilt}	Slip plane	Type	APB in (-111) ordering
1	[110]	a/2[011]	a/4[-110]	a/4[110]	a/2[001]	(1-11)	β	Yes
2	[110]	a/2[-101]	a/4[-110]	a/4[-1-10]	a/2[001]	(1-11)	β	Yes
3	[110]	a/2[-10-1]	a/4[-110]	a/4[-1-10]	a/2[00-1]	(-111)	β	No
4	[110]	a/2[01-1]	a/4[-110]	a/4[110]	a/2[00-1]	(-111)	β	No
5	[1-10]	a/2[01-1]	a/4[110]	a/4[-110]	a/2[00-1]	(111)	α	No
6	[1-10]	a/2[10-1]	a/4[110]	a/4[1-10]	a/2[00-1]	(111)	α	Yes
7	[1-10]	a/2[101]	a/4[110]	a/4[1-10]	a/2[001]	(-1-11)	α	No
8	[1-10]	a/2[011]	a/4[110]	a/4[-110]	a/2[001]	(-1-11)	α	Yes

Introducing an offcut to the (001) substrate used for growth introduces an asymmetry in the resolved shear stress on different {111} glide planes and to the misfit component of the Burgers vector of various 60° misfit dislocations making nucleation and glide of some of the misfit dislocations more favorable. (It also introduces an asymmetry in the glide path length for the dislocations on the different {111} glide planes from the growth surface to the interface that is also important). The effect of offcut on the misfit component of the Burgers vector is illustrated in figure 5 that shows for an (001) substrate, an offcut towards (-111) results in the dislocations gliding on (-111) having a larger misfit component to their Burgers vector and hence would be expected to nucleate and glide preferentially with respect to the misfit dislocations that glide on (1-11). As these two types of dislocation have tilt components in opposite directions, an imbalance in the numbers of misfit dislocations gliding on these

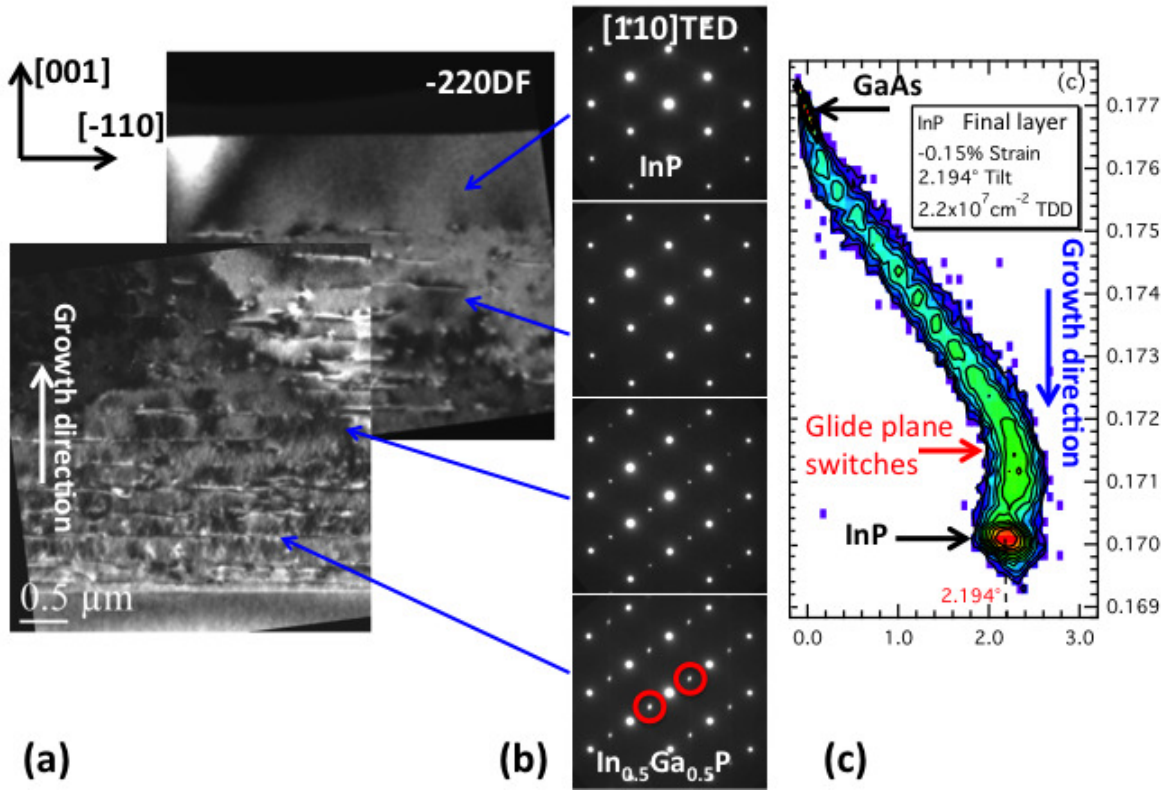

Figure 4. (a) -220 dark field (DF) image of InGaP graded buffer layer structure showing the misfit dislocation network. (b) [110] TED patterns from various parts of the graded buffer showing the absence of $CuPt_B$ atomic ordering at InGaP alloy compositions close to InP. (c) XRD RSM showing presence of unexpected direction of epitaxial layer tilt and a dislocation glide plane preference switch at an alloy composition close to InP.

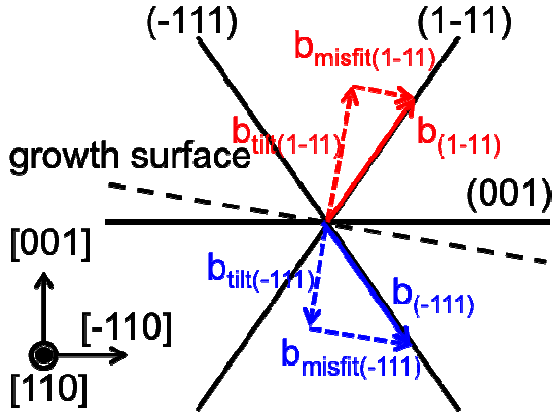

Figure 5. Diagram showing the effect of substrate offcut on the misfit component of the Burgers vector of two different 60° type dislocations gliding on (-111) and (1-11).

two different {111} planes will result in an overall epitaxial layer tilt that can be measured after growth using XRD. For the case of a compressively strained alloy layer grown on GaAs with the offcut illustrated in figure 5, the preferential nucleation and glide of misfit dislocations typically occurs on (-111) resulting in rotation of the lattice planes in the epitaxial layer towards the surface normal such that the average surface offcut becomes smaller [23–25].

However, in the case of the InGaP graded layers examined here, the substrate offcut introduces another asymmetry during the growth by preferentially selecting single variant $CuPt_B$ atomic ordering on (-111) planes, figure 6. A consequence of this is that glide of misfit dislocations on (1-11) planes leaves behind an antiphase boundary (APB) in the ordered structure whilst glide of misfit dislocations on (-111) does not, figure 6. As the $CuPt_B$ type ordering is metastable in the bulk, the formation of an APB in the single variant ordering in the crystal results in a reduction in energy and an energetic preference for nucleation and glide of misfit dislocations on (1-11) that outweighs the normal effect of the offcut. This we believe is the cause of the unusual epitaxial layer tilt behavior we observe in these graded InGaP buffer layers, figure 4. The glide plane switch occurs when the degree of ordering in the InGaP drops below a critical value as the alloy composition approaches InP resulting in a loss of the energetic preference for the nucleation and glide of misfit dislocations on (1-11) and a return to the more normally observed preference for nucleation and glide of misfit dislocations on (-111) planes for the sense of substrate offcut used. The introduction of new misfit dislocations gliding on (-111) planes naturally causes new threading dislocations resulting in the observed jump in the threading dislocation density for graded buffer layer structures grown beyond the point that the glide plane switch occurs.

To investigate this behavior further we have performed detailed transmission electron microscopy (TEM) and diffraction (TED) studies on a number of samples. Figure 7 shows ½{113} bright field (BF) and dark field (DF) images of the same area of the [110] cross-section of a single $In_{0.6}Ga_{0.4}P$ layer grown on a (001) GaAs substrate offcut 2° towards (-111). The inset TED pattern in figure 7(b) shows that this sample contained mostly domains of the (-111) variant of the atomic ordering as expected for the substrate offcut used. The superlattice dark field image of figure 7(b) exhibits contrast arising from two different types of APBs as reported previously [17, 18]. The wavy dark features rotated clockwise from the InGaP/GaAs interface are the naturally occurring

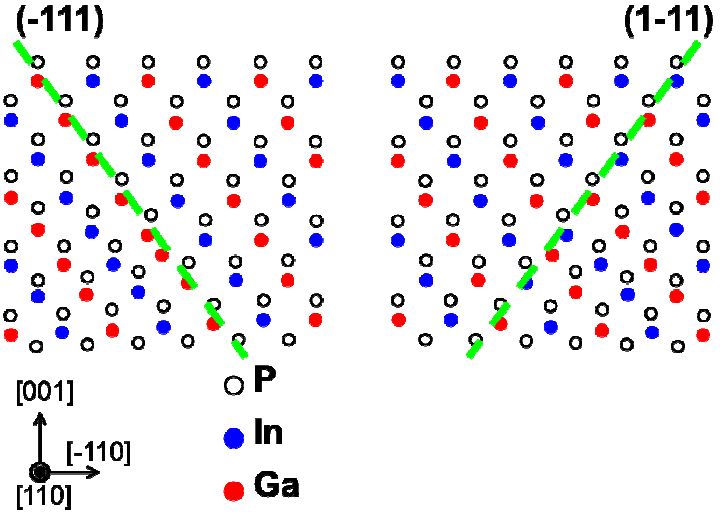

Figure 6. Schematic showing glide of 60° misfit dislocations on (-111) and (1-11) planes in (-111) ordered $In_{0.5}Ga_{0.5}P$. Glide on (1-11) planes results in an APB whilst glide on (-111) does not.

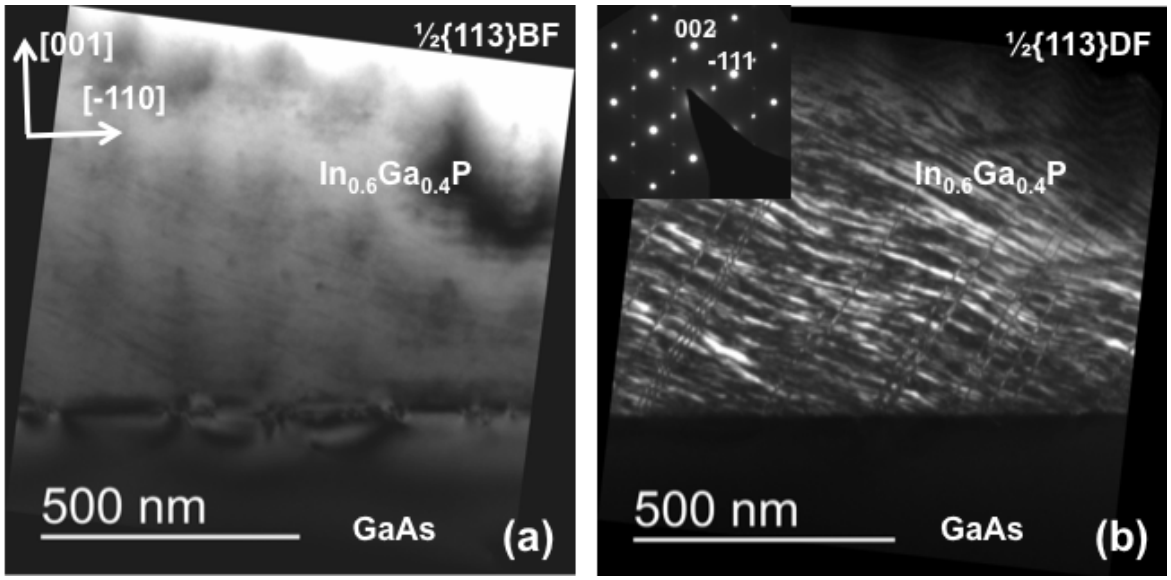

Figure 7. (a) ½{113} BF and (b) ½{113} superlattice DF images of (-111) ordered $In_{0.6}Ga_{0.4}P$ layer grown on (001) GaAs substrate offcut 2° towards (-111). Inset in (b) is the (110) TED pattern showing strong ½{111] superlattice spots arising from the ordering on (-111) planes. The dark field image of (b) shows two types of APBs as described in the text.

APDs in the ordered structure. The sharp, flat dark lines lying on (1-11) planes are APBs left behind by the glide of 60°, β-type misfit dislocations on this plane to the interface. Comparison with the bright field image of figure 7(a) reveals that all of the interfacial misfit dislocations left behind an APB in the ordered structure as observed previously by Spiecker et al in a similar sample [18]. No misfit dislocations were observed to have glided to the interface on (-111) planes consistent with the unusual direction of tilt observed in XRD studies of single variant atomically $CuPt_B$ ordered InGaP single layer and graded buffer layer samples. Further evidence of this was provided by high-resolution TEM studies of the misfit dislocations at the InGaP/GaAs interface. The vast majority of the dislocations were found to be dissociated into two partial dislocations with the stacking fault between them lying on the (1-11) glide plane, figure 8. The occurrence of dissociation of the misfit dislocations is useful as it enables identification of the glide plane for misfit dislocations even in a disordered sample. The above results are consistent with the XRD RSM obtained from this sample that revealed an epitaxial layer tilt of +0.3° indicating that glide on (1-11) planes was dominant.

In order to test whether the single variant $CuPt_B$ ordering is indeed responsible for the unusual dislocation glide plane preference and epitaxial tilt behavior observed in these samples, we have performed an experiment to remove the atomic ordering and see whether the dislocation glide plane preference switches back to that expected for the substrate offcut used. In this experiment, an Sb surfactant, known to disrupt or entirely prevent the $CuPt_B$ type atomic ordering [26, 27], was used during growth of the InGaP. The layer structure was the same as the sample illustrated in figures 7 and 8. [110] cross-section, high-resolution TEM studies of the misfit dislocations at this interface revealed the presence of misfit dislocations that had mainly glided in on (-111) planes, figure 9, indicating that after removing the single variant $CuPt_B$ atomic ordering the glide plane preference and epitaxial layer tilt returned to that normally expected for the direction of substrate offcut. Some residual ordering is visible at the InGaP/GaAs interface in figure 9 since on initiating growth of the InGaP it takes a while for the Sb surfactant surface concentration to build up to that required to eliminate the atomic ordering. The above results are consistent with the XRD RSM obtained from this sample that revealed an epitaxial layer tilt of -0.33° indicating that glide on (-111) planes was dominant.

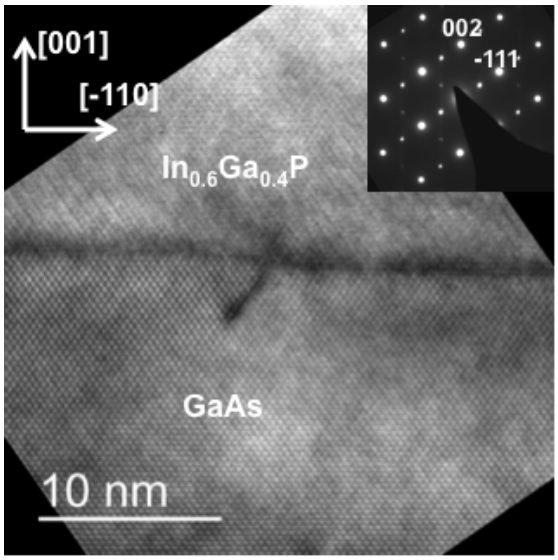

Figure 8. [110] cross-section, high-resolution TEM image showing interfacial misfit dislocation resulting from glide on (1-11) plane in a (-111) ordered InGaP layer grown on (001) GaAs substrate offcut 2° towards (-111) plane. Inset is the [110] TED pattern from the ordered InGaP layer.

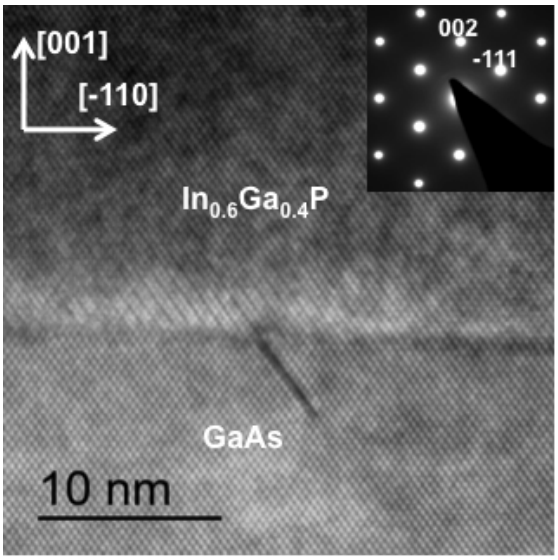

Figure 9. [110] cross-section, high-resolution TEM image showing interfacial misfit dislocation resulting from glide on (-111) plane in a random InGaP layer grown in the presence of Sb surfactant on (001) GaAs substrate offcut 2° towards (-111) plane. Inset is the [110] TED pattern from the random InGaP layer.

4. Discussion

Recent calculations indicate a substantial lowering in energy of the $CuPt_B$ InGaP ordered crystal by the introduction of an APB, giving rise to a strong preference for the glide of misfit dislocations with Burgers vectors that create an APB in this material [28]. The experimentally observed glide plane switch in the InGaP graded buffer layers occurs when the degree of atomic ordering falls below a critical value as the alloy composition approaches InP and nucleation and glide of misfit dislocations on the more normally reported (-111) plane for the substrate offcut used becomes energetically favorable and results in a substantial increase in the threading dislocation density. Although not presented in this paper, the presence of the single variant $CuPt_B$ atomic ordering also influences the glide of the α-type 60° misfit dislocations with line vectors along [1-10].

As well as affecting dislocation glide, the presence of atomic ordering will also influence the initial nucleation of misfit dislocations during growth of the graded buffer layers. As described by Marée et al [29], this is normally thought to occur at the layer surface by the nucleation of a dislocation half-loop, probably at the site of a stress concentrator such as a step bunch. The energy of a perfect dislocation half-loop E_{hl} of radius r is given by [29]

$$E_{hl} = E_l + E_s - E_\tau, \quad (1)$$

with

$E_l = [\mu b^2 r(1-\nu/2)/4(1-\nu)]\ln(\alpha r/b)$, $E_s = r\sigma_0 b\sqrt{3}$, and $E_\tau = \frac{1}{2}\pi r^2 \boldsymbol{\tau}\bullet\mathbf{b}$.

where E_l is the energy of a line dislocation of length πr, E_s is the energy associated with the creation of a surface step, and E_τ is the strain energy released by the loop. μ is the shear modulus, ν is Poisson's ratio, σ_0 the surface tension, b the magnitude of the Burgers vector, α is the dislocation core parameter, and τ is the magnitude of the resolved shear stress in the glide plane. In the case of nucleation of a dislocation half-loop on a {111} glide plane in the ordered InGaP with a Burgers vector such that it would create an APB, this introduces an extra energy lowering term in equation (1), $E_{APB} = \frac{1}{2}\pi r^2 \xi$, where ξ is the energy per unit area released by the formation of the APB such that equation (1) now becomes

$$E_{hl} = E_l + E_s - E_\tau - E_{APB} \quad (2)$$

This results in an energetic preference for the nucleation at the surface for misfit dislocation loops that generate an APB in the (-111) atomic ordering by reducing the critical radius and maximum energy required for nucleation of such half-loops over half-loops that do not generate an APB in the ordered structure.

In order to avoid a harmful increase in threading dislocation density associated with the observed glide plane switch during growth of the InGaP graded buffer layer, re-engineering of the buffer layer structure is required [30]. Further understanding of misfit dislocation nucleation and glide in these complex materials may enable control of the Burgers vector of the misfit dislocations to be achieved so as to enhance dislocation glide and promote favorable dislocation interactions to occur, leading to a reduced threading dislocation density in the final device.

5. Conclusions

The occurrence of single variant $CuPt_B$ atomic ordering during MOVPE growth of InGaP graded buffer layer structures on offcut (001) substrates has a profound influence on strain relaxation mechanisms in IMM solar cell structures. A strong preference is observed for the nucleation and glide of misfit dislocations that generate an APB in the ordered crystal, resulting in an epitaxial layer tilt in the opposite sense to that typically observed for the direction of substrate offcut used. As the alloy composition approaches InP, the reduction of atomic ordering leads to a switch in the glide plane preference back to that normally observed and the generation of new threading dislocations that harms device performance. The knowledge gained from these studies will enable the engineering of new graded buffer layer architectures resulting in higher efficiency devices.

Acknowledgements

The authors are pleased to thank W J Olavarria for growth of samples; K M Jones for FIB preparation of TEM samples; J M Olson, J Simon and M A Steiner for valuable discussions; and D J Friedman and M M Al-Jassim for technical leadership. This work is supported by the U.S. Department of Energy under Contract No. DE-AC36-08-GO28308 with the National Renewable Energy Laboratory.

References

[1] Sabnis V, Yuen H and Wiemer M 2012 *AIP Conf. Proc.* **1477** 14
[2] Wanlass M W, Ahrenkiel S P, Ahrenkiel R K, Albin D S, Carapella J J, Duda A, Geisz J F, Kurtz S, Moriarty T, Wehrer R J and Wernsman B 2005 *Proc. of the 31st IEEE PV Specialists Conference (Lake Buena Vista FL)* (Piscataway NJ: IEEE) p530
[3] King R R, Law D C, Edmondson K M, Fetzer C M, Kinsey G S, Yoon H, Sherif R A and Karam N H 2007 *Appl. Phys. Lett.* **90** 183516
[4] Geisz J F, Kurz S, Wanlass M W, Ward J S, Duda A, Friedman D J, Olson J M, McMahon W E, Moriarty T E and Kiehl J T 2007 *Appl. Phys. Lett.* **91** 023502
[5] Geisz J F, Friedman D J, Ward J S, Duda A, Olavarria W J, Moriarty T E, Kiehl J T, Romero M J, Norman A G and Jones K M 2008 *Appl. Phys. Lett.* **93** 123505
[6] Guter W, Schöne J, Philipps S P, Steiner M, Siefer G, Wekkeli A, Weiser E, Oliva E, Bett A W and Dimroth F 2009 *Appl. Phys. Lett.* **94** 223504
[7] Chiu P, Wojtczuk S, Zhang X, Harris C, Pulver D and Timmons M *Proc. of the 37th IEEE PV Specialists Conference (Seattle WA)* (Piscataway NJ: IEEE) p771
[8] Dimroth F and Kurtz S 2007 *MRS Bulletin* **32** 230
[9] Bremner S P, Levy M Y and Honsberg C B 2008 *Prog. Photovolt: Res. Appl.* **16** 225
[10] Geisz J F, Duda A, France R M, Friedman D J, Garcia I, Olavarria W, Olson J M, Steiner M A, Ward J S and Young M 2012 *AIP Conf. Proc.* **1477** 44
[11] Friedman D J 2010 *Current Opinion in Solid State and Mater. Sci.* **14** 131
[12] Beanland R, Dunstan D J and Goodhew P J 1996 *Advances in Physics* **45** 87
[13] Hirsch P B 1985 *Mats. Sci. Tech.* **1** 666

[14] Yonenaga I 1997 *J. de Physique III* **7** 1435
[15] Olsen J A, Hu E L, Lee S R, Fritz I J, Howard A J, Hammons B E and Tsao J Y 1995 *J. Appl. Phys.* **79** 3578
[16] Gomyo A, Suzuki T and Iijima S 1988 *Phys. Rev. Lett.* **60** 2645
[17] Baxter C S, Stobbs W M and Gibbings C J, 1993 *Phil. Mag. Lett.* **67** 59
[18] Spiecker E, Seibt M, Schröter W, Winterhoff R and Scholz F 2002 *Appl. Surf. Sci.* **188** 61
[19] Froyen S and Zunger A 1991 *Phys. Rev. Lett.* **66** 2132
[20] Bernard J E, Froyen S and Zunger A 1991 *Phys. Rev. B* **44** 11178
[21] Philips B A, Norman A G, Seong T-Y, Mahajan S, Booker G R, Skowronski M, Harbison J P and Keramidas V G 1994 *J. Cryst. Growth* **140** 249
[22] France R M, McMahon W E, Norman A G, Geisz J F and Romero M J 2012 *J. Appl. Phys.* **112** 023520
[23] Ayers J E, Ghandi S K and Schowalter LJ 1991 *J. Cryst. Growth* **113** 430
[24] Mooney P M, LeGoues F K, Tersoff J and Chu J O 1993 *J. Appl. Phys.* **75** 3968
[25] LeGoues F K, Mooney P M and Chu J O 1993 *Appl. Phys. Lett.* **62** 140
[26] Shurtleff J K, Lee R T, Fetzer C M and Stringfellow G B 1999 *Appl. Phys. Lett.* **75** 1914
[27] Stringfellow G B, Lee R T, Fetzer C M, Shurtleff J K, Hsu Y U, Jun S W, Lee S and Seong T-Y 2000 *J. Electron. Mater.* **29** 134
[28] McMahon W E, Kang J, France R M, Norman A G, Friedman D J and Wei S H 2013 *Appl. Phys. Lett*., submitted for publication
[29] Marée P M J, Barbour J C, van der Veen J F, Kavanagh K L, Bulle-Lieuwma C W T and Viegers M P A 1987 *J. Appl. Phys.* **62** 4413
[30] France R M, García I, McMahon W E, Norman A G, Simon J, Geisz J F, Friedman D J and Romero M J 2013 *IEEE J. Photovoltaics*, submitted for publication